Composite Structures 255 (2021) 113001

Contents lists available at ScienceDirect

Composite Structures

journal homepage: www.elsevier.com/locate/compstruct

# Resistance and ductility of FRP composite hybrid joints

Lulu Liu [a], Xin Wang [a,*], Zhishen Wu [a], Thomas Keller [b,*]

[a] Key Laboratory of C & PC Structures Ministry of Education, Southeast University, Nanjing 210096, China
[b] Composite Construction Laboratory (CCLab), École Polytechnique Fédérale de Lausanne (EPFL), Lausanne CH-1015, Switzerland

ARTICLE INFO

*Keywords:*
Bolted joint
Bonded joint
Hybrid joint
Resistance
Ductility
Efficiency
Displacement rate
Fail-safe condition

ABSTRACT

An experimental investigation of the load-bearing behavior and ductility of FRP hybrid double-lap joints composed of both adhesively-bonded and bolted connection parts was conducted. Amongst other things, the effects of the adherends' fiber architecture (uni- or multidirectional), adhesive type (stiff or flexible), and displacement rate were examined. The resistances of the hybrid joints with flexible adhesive corresponded to the full summation of the resistances of the bonded and bolted connection parts. The ultimate failure loads of these joints were furthermore significantly improved by increasing the displacement rate, while the deformation capacity did not decrease. The hybrid joints with multidirectional adherends and flexible adhesive exhibited high joint efficiencies and excellent ductility and thus may increase the overall safety of redundant engineering structures composed of brittle FRP members. These joints may also fulfill fail-safe conditions as required in European standards.

## 1. Introduction

Pultruded fiber-reinforced polymer (FRP) profiles have been the focus of increasing attention as structural members in recent structural engineering applications such as FRP truss structures or FRP bridge decks, because of their lightweight, superior mechanical- and durability-related properties and economical industrial production [1–3]. Since joints are usually the weakest part of load-bearing structures, effective joint design is the key to exploiting the full potential of FRP members. Joining is generally done by adhesive bonding or mechanical bolting [4]. Adhesively-bonded joints normally exhibit higher stiffness and efficiency than bolted joints and can easily connect different materials and geometries; however, they are sensitive to the fabrication process and difficult to implement on-site [5]. Although bolted joints are easier to assemble and disassemble, there are concerns about durability since the FRP materials are drilled [6]. With the intention of combining the advantages offered by these two joint techniques, hybrid joints, i.e. bonded-bolted joints, have attracted increasing interest in different fields of application [7].

A controversial aspect of hybrid joints is whether or not the resistances of the combined bonded and bolted connections can be summed. In the first studies, relatively stiff adhesives were used compared to the stiffness of the bolted connection and no load-sharing was observed. Hybrid joints were thus only suggested for fail-safe, i.e. damage-tolerant designs, where the bolted connection should bear the load in case of bond failure [8]. Similar results were obtained in [9–12], i.e. hybrid joints did not improve the bonded joint resistance. Design guidelines were established accordingly [13], and applied, e.g. for the design of the Pontresina bridge, constructed in Switzerland in 1997 [14], where bolts were inserted into the epoxy adhesive connections as a back-up system to prevent bridge collapse in case of bond failure. More recently, a certain degree of load sharing between bonded and bolted connections was however achieved by using more flexible adhesives, i.e. by approaching the adhesive connection stiffness to that of the bolted connection [15–19], or by reducing the bolt clearance, i.e. increasing the stiffness of the bolted connection [11,20].

Although several investigations have been carried out of hybrid joints with improved load- sharing behavior, a full summation of the bonded and bolted connection resistances has not yet been achieved. The investigation of hybrid joints also often focused on applications in the aerospace industry where neat-fit bolts with minimal clearance are preferred, while in structural engineering applications the clearances are significantly larger due to tolerance requirements; the results of the former are thus not applicable to the latter. Furthermore, significant structural aspects of hybrid joints incorporating flexible adhesives have not yet been addressed, such as the potential ductility, i.e. the ability to dissipate inelastic energy, and the loading or displacement rate on which the deformation capacity of the adhesive layer may strongly depend. The aims of the present work are therefore 1) to achieve a full summation of the bonded and bolted connection resis-

* Corresponding authors.
*E-mail addresses:* xinwang@seu.edu.cn (X. Wang), thomas.keller@epfl.ch (T. Keller).

https://doi.org/10.1016/j.compstruct.2020.113001
Received 4 August 2020; Revised 17 September 2020; Accepted 19 September 2020
Available online 24 September 2020

tances in hybrid joints by appropriate selection of adhesive and adherend materials, 2) to systematically evaluate the performance of hybrid joints regarding joint resistance, ductility, and displacement rate, and 3) to provide guidelines regarding fail-safe and ductile designs.

The work thus experimentally investigated the effects of the bonded and bolted connection behavior on the resistance and ductility of hybrid, i.e. combined bonded-bolted joints, to obtain optimum hybrid combinations. Two different adhesives (a stiff one and a flexible one) and two different FRP adherends (with uni- and multidirectional architectures) were selected. The displacement rate was varied and loading–unloading-reloading cycles were performed to evaluate the ductility of selected bolted, bonded and hybrid joints. Different compositions of hybrid joints were derived to meet fail-safe and/or ductility requirements in line with European standards.

## 2. Experimental program

The experimental work comprised three main objectives, 1) to study the effects of fiber architecture and bolt diameter on the bolted joint behavior, and the effects of the adhesive type, displacement rate, layer thickness and overlap length on bonded joint behavior, to provide references for their combinations in hybrid joints; 2) to investigate the effects of fiber architecture, adhesive type and displacement rate on the resistance and ductility of hybrid joints, to determine the most effective combination; and 3) to further investigate the conditions required for hybrid joints to be fail-safe.

### 2.1. Materials

Basalt-FRP (BFRP) pultruded plates were used as adherends because of their excellent mechanical and chemical properties, and environmentally friendly characteristics compared to glass-FRP (GFRP) [21,22]; the plate thickness was 4.15 mm. Two different fiber architectures were considered, designated UD and MD. The UD plates were pultruded with unidirectional (UD) basalt fiber rovings of 1200-tex and impregnated with Aradur 1562-1 epoxy resin; the MD plates were composed of the same basalt rovings and multi-directional (MD) basalt fabrics (0°/45°/−45°/90°), with an area density of 600 g/m$^2$. Five layers of MD fabrics were selected to optimize the integral structural performance of members and joints in truss applications, i.e. to provide a high joint performance without however excessively affecting the axial member stiffness [23]. Both fiber architectures were symmetrical, as shown in Fig. 1. The total fiber volume fractions were 66% (UD) and 68% (MD) determined by resin burn-off according to ASTM 3171; in the latter case, the volume fractions according to the directions of the fiber orientation were 0°/±45°/90° = 70/20/10%. Basalt fibers, fabrics and BFRP pultrusions were manufactured and provided by Jiangsu GMV Co. Ltd, China. The basic mechanical properties of the constituent materials, provided by the manufacturer, and BFRP adherends, obtained from tensile experiments according to ASTM 3039, are listed in Table 1.

Stainless steel, 12.9-grade bolts with 1080 MPa yield strength and 1200 MPa ultimate strength were selected and an acrylic and an epoxy adhesive were used. The acrylic adhesive (SikaFast 5221 NT [24]) is based on Acrylic Double Performance technology, designated ADP in the following, and is flexible and exhibits high failure strain. The epoxy adhesive (Sikadur 330 [25]), designated EP, is comparably stiff, has low failure strain and is commonly used for structural bonding. The mechanical properties of these two adhesives were investigated in [26] and [27], respectively, and selected values are listed in Table 1.

### 2.2. Specimen geometry and preparation

Symmetric double-lap joints were considered to minimize the effects of the load eccentricity according to [28]. The joint adherends were cut from the pultruded BFRP plates; the specimen dimensions of the bonded and hybrid joints were derived from the design of the bolted joints with 8-mm bolt diameter, as shown in Fig. 2.

To prevent the premature failure of the bolted joints, the geometrical requirements according to [13] were fulfilled to obtain bearing failure, i.e. the ratio of adherend width-to-bolt diameter ($w/d$) was selected as 4.5 and the end distance-to-bolt diameter ($e_1/d$) as 4.0, see Fig. 2(a). Four bolt diameters were considered for MD joints, namely, 4, 6, 8 and 10 mm, while only 8-mm bolts were used for the UD joints. Pre-tightening of 1 Nm was applied by a torque wrench to simulate finger-tightened conditions, i.e. to represent the worst case of a bolt losing an initial higher torque due to creep. The bolt clearance was set to approximately 4% of $d$, namely, 0.1, 0.2, 0.3 and 0.4 mm for the four bolt diameters.

Two adhesive thicknesses (1 and 2 mm) and two overlap lengths (64 and 136 mm) were used for the bonded joints, as shown in Fig. 2(b). They were manufactured in three main steps: surface preparation, bonding and curing. The adherend surfaces were abraded using an automatic sanding machine with 60-grit abrasive paper to remove release agent and surface resin until the fibers appeared at approximately 0.1-mm depth. The bonding area was then cleaned with a cleaning and activating agent (Sika ADPrep) developed for this adhesive. Specimens comprising the EP adhesive were ready for the next step of bonding. In ADP specimens, based on previous experiences [29,30], a promotor, i.e. 0.1-mm-thin layer of EP adhesive, was further applied and cured at 60 °C for four hours. The promoter layer was then slightly abraded using 80-grit abrasive paper to provide a rough surface for the ADP adhesive. The alignment of the joints was assured by an in-house developed fixture and several glass balls were dispersed on the fresh adhesive to guarantee the adhesive thickness. After fabrication, weights were placed on the joints to provide pressure during the curing process. All specimens were cured under ambient laboratory conditions at around 20 ± 2 °C for seven days.

In all hybrid joints 8-mm diameter bolts, 2-mm adhesive layer thickness, and 64-mm overlap length were used, as shown in Fig. 2 (c); the joints were manufactured in two steps. Firstly, bonded joints were fabricated and cured as described above. A hole was then drilled in the center of the bonded area and the bolt was inserted and tightened by the torque wrench, as for the bolted joints. The hole was thus drilled after bonding to provide uniform clearance conditions through the adherends.

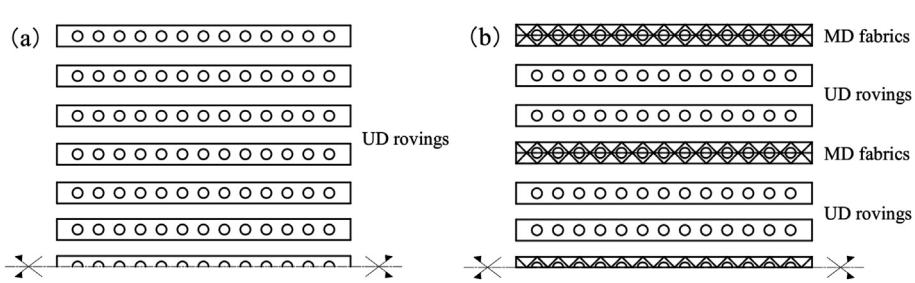


**Fig. 1.** Fiber architecture of (a) UD and (b) MD adherends.

**Table 1**
Mechanical properties of constituent materials, BFRP adherends and adhesives.

| Materials | Mechanical properties | | |
|---|---|---|---|
| | Tensile strength (MPa) | Tensile modulus (GPa) | Failure elongation (%) |
| Basalt fiber rovings | 2100 | 91 | 2.30 |
| Aradur 1562-1 epoxy | 6 ± 2 | 2.8 ± 0.25 | 2.65 ± 0.32 |
| UD adherends | 1212 ± 23 | 51.4 ± 0.9 | 2.36 ± 0.02 |
| MD adherends | 971 ± 25 | 41.7 ± 1.8 | 2.33 ± 0.04 |
| ADP adhesive[(a)] | 12 ± 4.3 | 0.21 ± 0.05 | 59.8 ± 14.5 |
| EP adhesive | 38 ± 2.1 | 4.6 ± 0.14 | 0.83 ± 0.13 |

[(a)] ASTM D638 set-up, 2 mm/min displacement rate [26].

An overview of the series of bolted, bonded and hybrid joint configurations is given in Table 2. The designation for the joints is as follows: B/A/H-U/M-4/6/8/10/E/A/E8/A8-1/10/100-1/2-64/136, where B/A/H designates bolted/adhesive/hybrid; U/M designates UD/MD adherends; 4/6/8/10/E/S/E8/S8 indicates bolt diameter and adhesive type (E for EP and A for ADP); 1/10/100 indicates displacement rate in (mm/min) (see below); 1/2 indicates adhesive layer thickness; and 64/136 the overlap length. Three specimens were investigated for each configuration.

### 2.3. Experimental set-up, instrumentation and procedure

All experiments were conducted on a computer-controlled machine (universal machine $w + b$ 200 kN with maximum stroke of 200 mm) at laboratory temperature (15 ± 5 ℃). Monotonic tensile loading was applied while loading–unloading-reloading cycles were performed for selected specimens, according to Table 2. In the latter case, the unloading cycles were performed after significant yielding (ADP adhesive) or damage (bolt bearing) but prior to the joints' ultimate failure loads. After unloading to 0 kN at the same displacement rate as during loading, the bolted joints were directly subjected to reloading up to failure, while for the ADP bonded and hybrid joints, prior to reloading, the loads were sustained at 0 kN for 1 h to observe the delayed recovery deformation. Displacement control at a rate of 1 mm/min was used, except for two ADP bonded and hybrid configurations, where the rate was increased to 10 mm/min and 100 mm/min, see Table 2. The load and vertical stroke of the machine were recorded at a 2-Hz frequency by a DOLI EDC 60/120 data-acquisition device. A video extensometer camera was used to measure the joint displacements during loading and capture images of the specimens at regular intervals. 3 × 3 black speckles were marked on the specimens' lateral surfaces, as shown in Fig. 3. The in-plane coordinates of these targets were monitored at a 2-Hz frequency by a LabVIEW application. The joint displacements were determined in the joint area from the average values of the $u(2)$-$u(7)$ and $u(2)$-$u(9)$ displacements, as shown in Fig. 3.

## 3. Experimental results and discussion

### 3.1. Bolted joints

#### 3.1.1. Effects of fiber architecture

The effects of fiber architecture UD and MD on the load–displacement responses of the bolted joints are shown in Fig. 4 (selected representative specimens for each case). Compared to the UD configuration, bolted joints with MD fiber architecture exhibited significantly (almost two times) increased ultimate failure loads and much larger deformation capacity, i.e. ultimate deformations, as listed

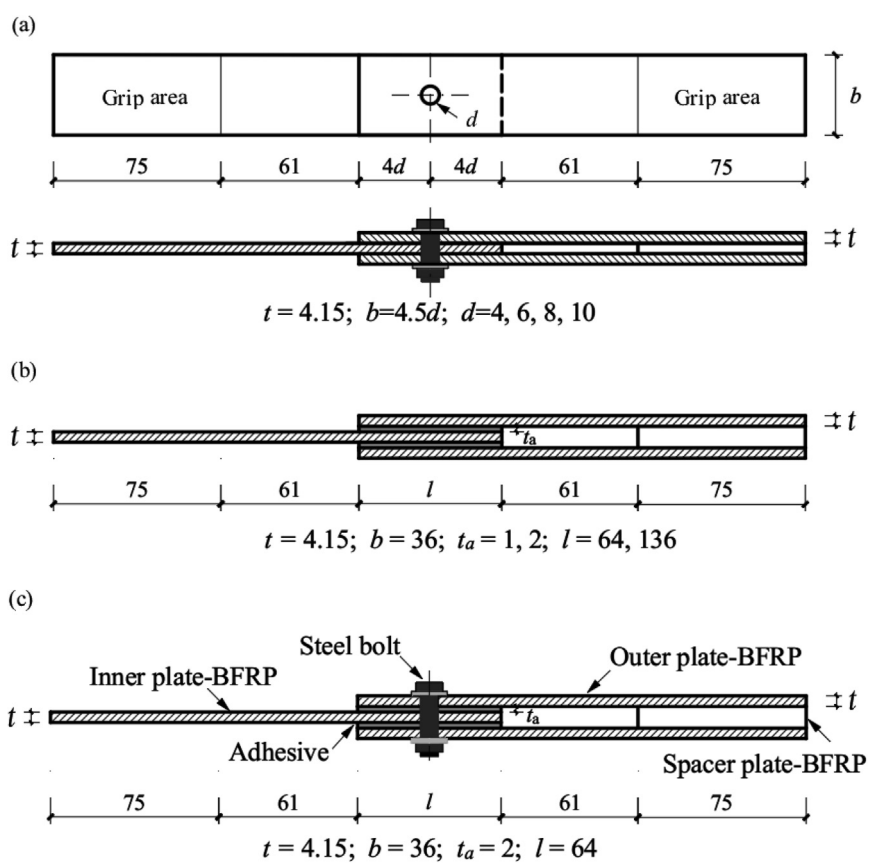


**Fig. 2.** Joint dimensions: (a) bolted joint; (b) bonded joint; (c) hybrid joint (dimensions in (mm)).

**Table 2**
Overview of experiments for joint configurations.

| Joint type | Specimen denomination | Adherend | Adhesive | Bolt diameter (mm) | Displ. Rate (mm/min) | Adhesive thickness (mm) | Overlap length (mm) |
|---|---|---|---|---|---|---|---|
| Bolted joints | B-U-8 | UD | – | 8 | – | – | 64 |
| | B-M-4 | MD | – | 4 | – | – | 64 |
| | B-M-6 | MD | – | 6 | – | – | 64 |
| | B-M-8[(a)] | MD | – | 8 | – | – | 64 |
| | B-M-10 | MD | – | 10 | – | – | 64 |
| Adhesively- bonded joints | A-U-E-1-2-64 | UD | EP | – | 1 | 2 | 64 |
| | A-U-A-1-2-64 | UD | ADP | – | 1 | 2 | 64 |
| | A-M-E-1-2-64 | MD | EP | – | 1 | 2 | 64 |
| | A-M-E-1-2-136 | MD | EP | – | 1 | 2 | 136 |
| | A-M-A-1-1-64 | MD | ADP | – | 1 | 1 | 64 |
| | A-M-A-1-2-64[(a)] | MD | ADP | – | 1 | 2 | 64 |
| | A-M-A-1-2-136 | MD | ADP | – | 1 | 2 | 136 |
| | A-M-A-10-2-64 | MD | ADP | – | 10 | 2 | 64 |
| | A-M-A-100-2-64 | MD | ADP | – | 100 | 2 | 64 |
| Hybrid joints | H-U-E8-1-2-64 | UD | EP | 8 | 1 | 2 | 64 |
| | H-U-A8-1-2-64 | UD | ADP | 8 | 1 | 2 | 64 |
| | H-M-E8-1-2-64 | MD | EP | 8 | 1 | 2 | 64 |
| | H-M-A8-1-2-64[(a)] | MD | ADP | 8 | 1 | 2 | 64 |
| | H-M-A8-10-2-64 | MD | ADP | 8 | 10 | 2 | 64 |
| | H-M-A8-100-2-64 | MD | ADP | 8 | 100 | 2 | 64 |

[(a)] Third specimen was subjected to loading–unloading-reloading cycles.

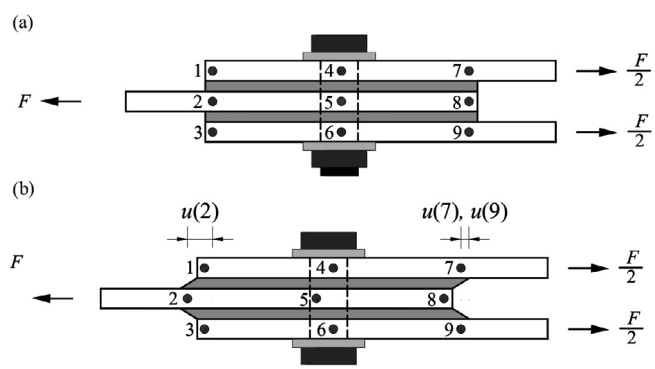


**Fig. 3.** Position of video-extensometer measurement points on hybrid joint: (a) initial; (b) deformed stage.

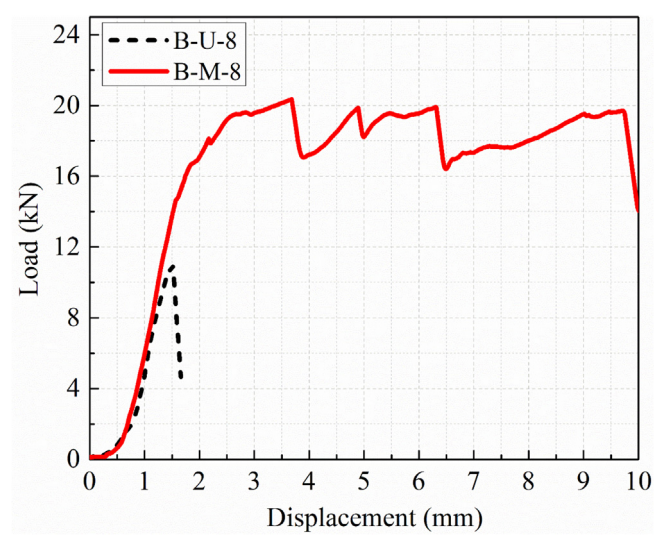


**Fig. 4.** Load-displacement responses for bolted joints with different fiber architectures.

in Table 3. The improved joint behavior was attributed to a change in failure mode from an early and brittle splitting failure in the UD case to a progressive bearing failure in the MD joints, as shown in Fig. 5. In the UD case, adherend splitting started from the local bearing point and propagated to the free edge in a sudden and brittle manner. In the MD case, the progressive crushing of the adherend in front of the hole activated the 45°- and 90°-plies and thus prevented splitting failure and enabled dissipation of inelastic energy and an associated (pseudo-)ductile behavior.

### 3.1.2. Effects of bolt diameter

The effects of varying bolt diameters on the load–displacement responses of joints comprising MD adherends are shown in Fig. 6. The ultimate failure loads and deformation capacity were improved when the bolt diameter was increased from 4 mm to 10 mm. This increase could be attributed to the also increasing end distances and thus lengths of possible bearing failure, see Fig. 7, which shows the bearing failure modes. In the case of the smallest 4-mm diameter, shear failure occurred in the steel bolt prior to any significant development of bearing failure (see Fig. 7).

The bearing strength, $\sigma_{b,ult}$, was obtained as follows:

$$\sigma_{b,ult} = \frac{F_{ult}}{d \cdot t} \tag{1}$$

where $F_{ult}$ is the joint ultimate failure load, $d$ is the bolt diameter and $t$ is the adherend thickness.

In contrast to the ultimate failure load, the bearing strength was almost independent of the bolt diameter, with only a small decrease being exhibited with increasing diameter, as shown in Fig. 8.

## 3.2. Bonded joints

### 3.2.1. Effects of adhesive type

The load–displacement behavior of both ADP and EP bonded joints was hardly affected by the adherends' fiber architecture (UD or MD), see Table 3, and thus only the results of the MD cases are presented in the following. The effects of the adhesive type on the load–displacement responses are shown in Fig. 9 for the 64-mm overlap length. The EP specimens exhibited a linear and brittle behavior while the ADP

**Table 3**
Summary of experimental results for joint configurations.

| Joint type | Specimen denomination | Yield displacement (mm) | Yield load (kN) | Ult. failure displacement (mm) | Ult. Failure load (kN) |
|---|---|---|---|---|---|
| Bolted joints | B-U-8 | – | – | 1.56 ± 0.07 | 11.0 ± 0.2 |
| | B-M-4 | 2.42 ± 0.18 | 10.5 ± 0.3 | 2.75 ± 0.31 | 10.7 ± 0.2 |
| | B-M-6 | 2.98 ± 0.37 | 14.4 ± 0.3 | 5.72 ± 0.38 | 16.3 ± 0.2 |
| | B-M-8 | 3.10 ± 0.42 | 19.5 ± 0.8 | 9.45 ± 0.21 | 20.9 ± 0.4 |
| | B-M-10 | 4.23 ± 0.93 | 21.0 ± 0.6 | 17.05 ± 0.71 | 24.6 ± 0.5 |
| Adhesively- bonded joints | A-U-E-1-2-64 | –- | –- | 0.012 ± 0.004 | 19.3 ± 1.0 |
| | A-U-A-1-2-64 | 0.35 ± 0.02 | 25.8 ± 0.6 | 5.48 ± 0.32 | 43.7 ± 1.3 |
| | A-M-E-1-2-64 | – | – | 0.012 ± 0.003 | 18.0 ± 0.6 |
| | A-M-E-1-2-136 | – | – | 0.017 ± 0.005 | 26.0 ± 0.6 |
| | A-M-A-1-1-64 | 0.25 ± 0.01 | 33.5 ± 2.3 | 2.94 ± 0.04 | 56.3 ± 3.4 |
| | A-M-A-1-2-64 | 0.34 ± 0.02 | 26.1 ± 0.7 | 5.39 ± 0.49 | 41.2 ± 1.3 |
| | A-M-A-1-2-136 | 0.73 ± 0.13 | 56.0 ± 0.8 | 5.85 ± 0.54 | 92.4 ± 6.5 |
| | A-M-A-10-2-64 | 0.42 ± 0.034 | 33.7 ± 2.4 | 5.26 ± 0.25 | 47.4 ± 2.9 |
| | A-M-A-100-2-64 | 0.45 ± 0.015 | 43.7 ± 0.8 | 6.92 ± 0.52 | 51.0 ± 2.4 |
| Hybrid joints | H-U-E8-1-2-64 | – | – | 2.02 ± 0.079 | 26.7 ± 1.8 |
| | H-U-A8-1-2-64 | 0.33 ± 0.04 | 25.4 ± 0.9 | 5.28 ± 0.44 | 39.3 ± 3.0 |
| | H-M-E8-1-2-64 | – | – | 9.52 ± 1.47 | 23.3 ± 1.4 |
| | H-M-A8-1-2-64 | 0.39 ± 0.03 | 24.01 ± 1.2 | 5.24 ± 0.13 | 56.8 ± 3.4 |
| | H-M-A8-10-2-64 | 0.42 ± 0.11 | 26.3 ± 1.0 | 5.56 ± 0.05 | 61.5 ± 3.5 |
| | H-M-A8-100-2-64 | 0.48 ± 0.03 | 43.4 ± 1.4 | 5.58 ± 0.74 | 66.0 ± 2.2 |

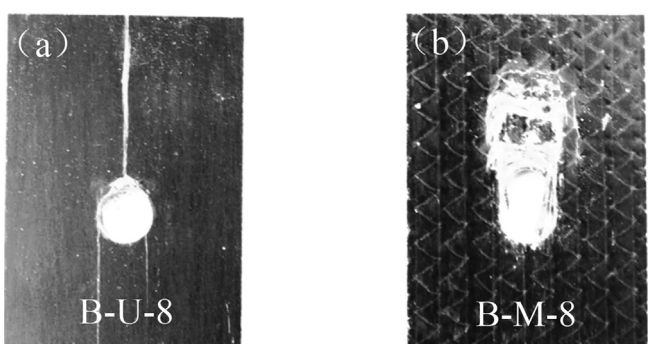


**Fig. 5.** Failure modes for bolted joints with different fiber architectures: (a) UD splitting failure; (b) MD bearing failure.

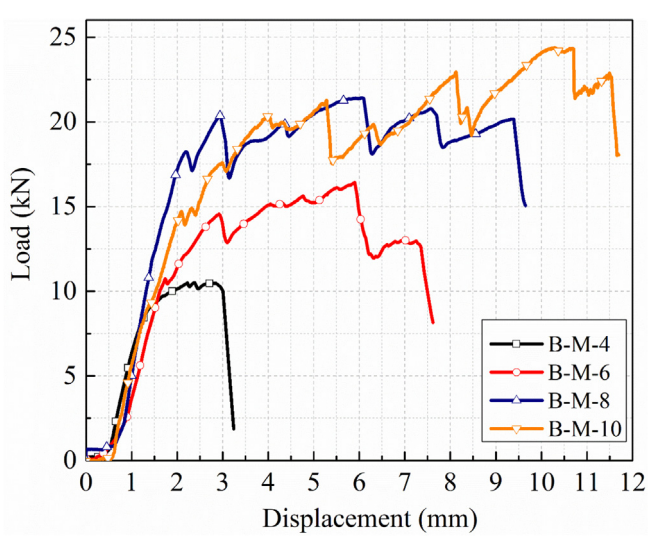


**Fig. 6.** Load-displacement responses of MD bolted joints with different bolt diameters.

specimens showed a bilinear and highly ductile response (also see below). Linear elastic behavior was observed up to 64% (on average) of the ultimate failure load, followed by a yield behavior and subsequent slight hardening, attributed to the stretching of the molecular chains [26,30]. In addition to the much higher deformation capacity, the ultimate failure load of the ADP joint was 2.3x higher (on average) than that of the EP joints.

The failure modes of these two adhesively-bonded joint types are shown in Fig. 10. Crack initiation always occurred at the end of the overlap edges and the crack then propagated inwards up to the ultimate failure, as recorded by the video camera. Different failure surfaces were observed; the EP joints exhibited a mixed failure dominated by adhesive failure (according to ASTM 5573), i.e. failure in the adhesive-adherend interface, but also with a significant proportion of light-fiber-tear failure. ADP joints exhibited two failure modes, either a mixed failure of cohesive failure (in the adhesive) and light-fiber-tear failure, or predominate cohesive failure, the latter associated with a slightly lower ultimate failure load.

### 3.2.2. Effects of displacement rate

The effect of the displacement rate on the load–displacement responses of ADP bonded joints are shown in Fig. 11 for 1.0, 10 and 100 mm/min, respectively. The yield and ultimate failure loads improved with the increasing displacement rate, while the former showed a more significant shift upwards than the later since hardening at lower rates was more significant, i.e. the molecule network had more time to align to the loading direction. However, the varying displacement rate hardly affected the initial stiffness, and yield and ultimate failure displacements. The failure mode was a mixed cohesive/light-fiber-tear failure that did not change at higher rates.

### 3.2.3. Effects of adhesive layer thickness

The effects of the adhesive layer thickness on the load–displacement behavior of the ADP bonded joints are shown in Fig. 12, thicknesses of 1 mm and 2 mm are compared for 64-mm overlap length. Both responses were almost bilinear and ductile. The ultimate failure loads of the 2-mm adhesive joints were 25% lower (on average) than those of the 1-mm layer joints due to the higher eccentricity in the former, which increased the through-thickness tensile stresses. The deformation capacity however increased significantly and was almost proportional to the thickness ($t_a$) since the shear deformation ($\Delta$) was proportional to the latter, as shown in the top right corner of Fig. 12. The hardening in the post-yield stage, i.e. the stretching of the molecular chains, was much more pronounced for the thinner layer. Only one failure mode was observed for the 1-mm bonded joints, i.e. mixed cohesive/light-fiber-tear failure.

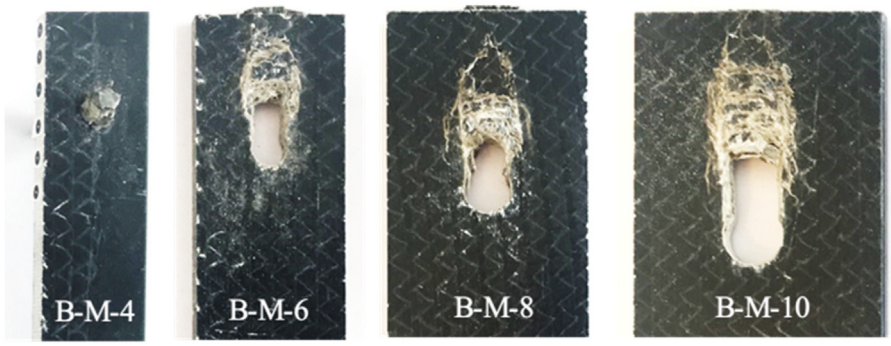


**Fig. 7.** Failure modes of MD bolted joints with different bolt diameters.

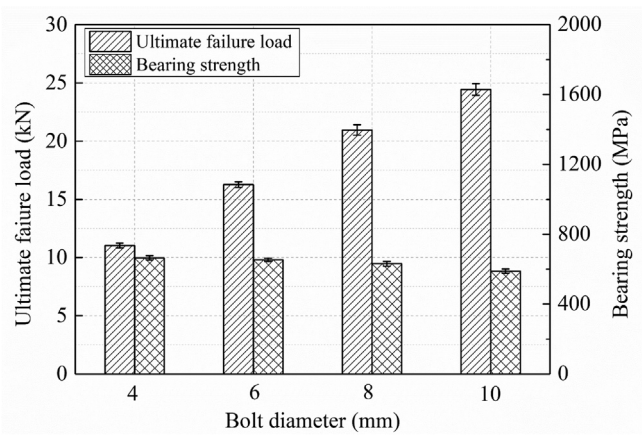


**Fig. 8.** Ultimate failure loads and bearing strengths of MD bolted joints with different bolt diameters (av. values and standard deviation bars).

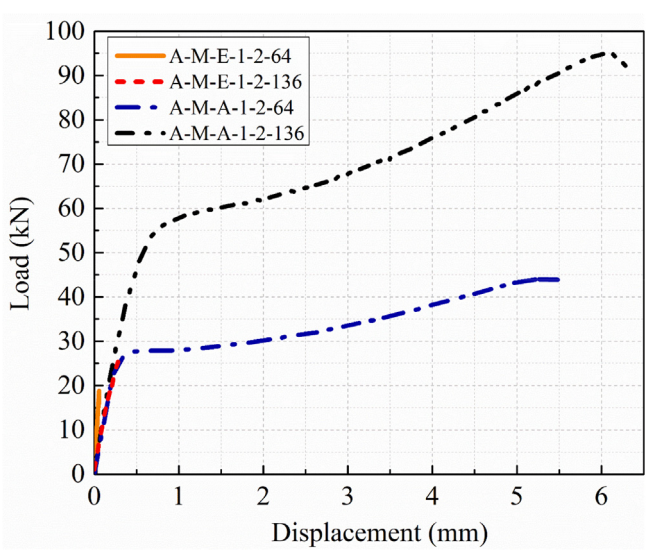


**Fig. 9.** Load-displacement responses of bonded joints with two types of adhesives and different overlap lengths.

#### 3.2.4. Effects of overlap length

The effects of the adhesive overlap length on the load–displacement responses of EP and ADP bonded joints are shown in Fig. 9. The ultimate failure loads of the EP joints with $l$ = 136 mm were slightly higher than with $l$ = 64 mm, but increased much less than proportionally to the overlap length. The yield and ultimate failure loads of the ADP joints, in contrast, increased almost linearly with the overlap length, as shown in Table 3; the post-yield curves were basically shifted upwards, although the hardening increased slightly for the longer lengths. Typical for relatively stiff adhesives, the behavior of the EP joints was dominated by combined shear and through-thickness tensile stress peaks at the edges which prevented a significant increase of the ultimate loads if the overlap length was increased [13]. In the ADP joints however, since the ultimate loads increased almost linearly with the overlap length, a primarily uniform shear stress distribution must have governed the behavior [13]. The failure modes of the EP and ADP bonded joints with 136-mm overlap length were similar to those in the previous cases, see Fig. 13.

### 3.3. Hybrid joints

#### 3.3.1. UD-EP hybrid joints

The load–displacement response of a typical UD-EP hybrid joint comprising UD adherends and EP adhesive is shown in Fig. 14 and compared with corresponding typical UD bolted and EP bonded joints. The hybrid joint exhibited two sequential stages in the load–displacement response. In the first stage, the applied load was transferred solely by the adhesive connection due to its much higher stiffness compared to the bolted connection, which first had to compensate the 0.3-mm clearance. Subsequently, adhesive failure occurred and the load dropped to the level of the bolted joint at this displacement, i.e. almost 0 kN. In the second stage, the hybrid joint response approached that of the bolted joint, i.e. the load increased again, at a much lower stiffness, until splitting failure occurred as in the UD bolted joint, at a much lower load however compared to the previous peak. The slightly higher peak load in the first and higher stiffness in the second stage exhibited by the hybrid joint, compared to the bonded and bolted joints, can be explained by friction caused by the slight bolt clamp (1st stage) and the rough adhesive fracture surfaces (2nd stage). The typical failure mode of the UD-EP hybrid joints is shown in Fig. 15 (a), exhibiting light-fiber-tear and splitting failures, i.e. a combination of the failure modes of the EP bonded and UD bolted joints.

#### 3.3.2. UD-ADP hybrid joints

The load–displacement response of a representative UD-ADP hybrid joint comprising UD adherends and ADP adhesive is shown in Fig. 16 and compared with the responses of a UD bolted and ADP bonded joint. Similarly to the UD-EP hybrid joint, the bolted connection was not loaded initially. As the relative displacement between the adherends was increased, i.e. the ADP adhesive had entered the yield stage, the bolted connection started however to share the load. As a result, the load in the hybrid joint became the linear summation of the bonded and bolted connections and the behavior became stiffer, up to a first peak, where a shear-out failure occurred in the adherend,

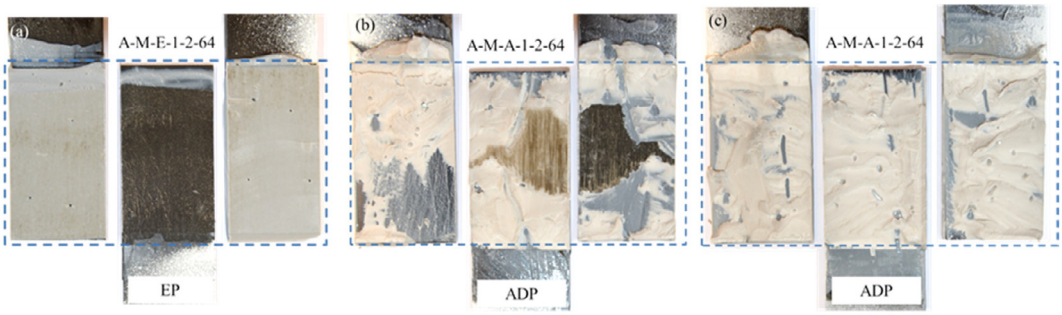


**Fig. 10.** Failure modes for two types of adhesives: (a) mixed adhesive/light-fiber-tear failure for EP; (b) mixed cohesive/light-fiber-tear failure for ADP; (c) predominant cohesive failure for ADP.

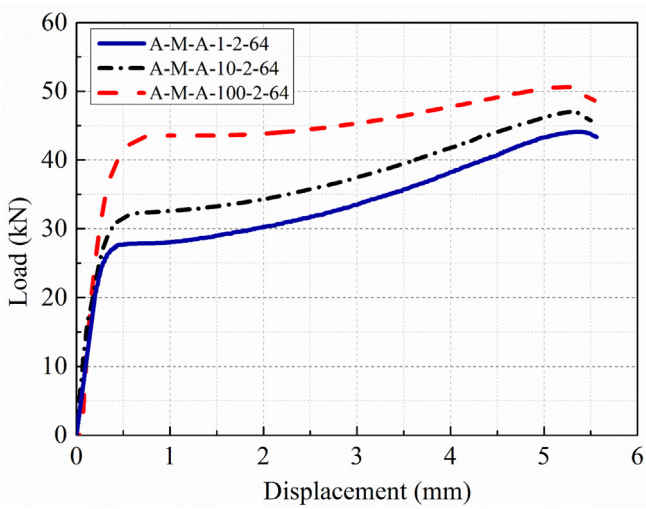


**Fig. 11.** Load-displacement responses of ADP bonded joints at different displacement rates.

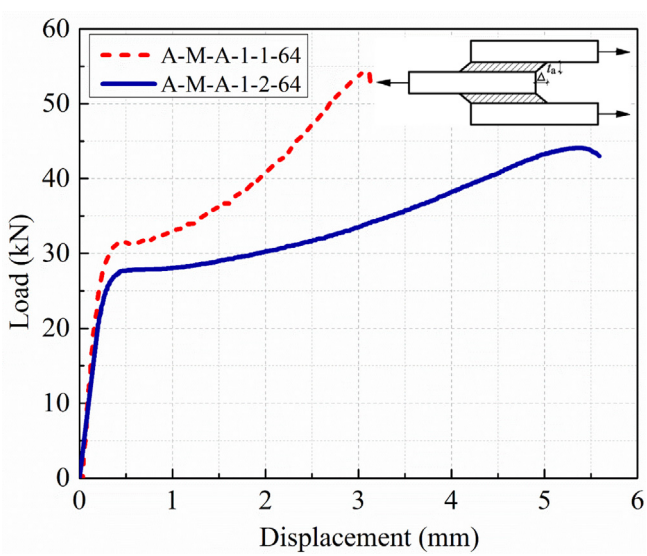


**Fig. 12.** Load-displacement responses of ADP bonded joints with different adhesive thicknesses.

as shown in Fig. 15(b). After a drop of the load to the approximate level of the corresponding bonded joint, the bonded connection continued to transfer the load until the ultimate load was reached, when a predominant cohesive failure occurred in the adhesive. Since the ultimate failure load of the bolted UD connection was much lower than that of the bonded connection, the resistance of the UD-ADP hybrid joint did not significantly improve compared to the ADP bonded joint although full load sharing occurred.

### 3.3.3. MD-EP hybrid joints

The load–displacement response of a typical MD-EP hybrid joint comprising MD adherends and EP adhesive is shown in Fig. 17 and compared with corresponding MD bolted and EP bonded joints. The hybrid joints exhibited a similar two-stage behavior as the previously discussed UD-EP hybrid joints, i.e. no load sharing between the bonded and bolted connections occurred. After failure of the bonded connection (exhibiting a light-fiber-tear failure), the entire load was transferred by the bolt and the ultimate failure load increased up to the adherend's bearing strength at large deformations, see bearing failure mode in Fig. 15(c). Since the MD bolted connection exhibited a load capacity almost equal to that of the bonded connection, the former could be considered as a redundant load path in case of bonded connection failure and thus would fulfill the fail-safe condition required for bonded joints according to [28], see following discussion.

### 3.3.4. MD-ADP hybrid joints

The load–displacement response of a representative MD-ADP hybrid joint, composed of MD adherends and ADP adhesive, is compared to the responses of MD bolted and ADP bonded joints in Fig. 18; all joints exhibited a ductile behavior (see below) with large deformation capacity. Until the bolted connection was activated, the stiffness of the hybrid joint was governed by the bonded connection, and no load sharing had yet occurred. Subsequently, full load sharing initiated and continued and joint stiffness increased accordingly up to the ultimate failure load, which was almost the summation of the bonded and bolted connection resistances (see mean values in Table 3, −8.7%) and was reached at large deformations. Taking however the increasing hole in the adhesive layer into account, a full summation of the individual connection resistances was obtained. After failure of the adhesive connection, the load dropped to the level of the bolted connection, which continued to sustain the load until its ultimate failure. The failure mode of the MD-ADP hybrid joints consisted of a predominant cohesive failure in the adhesive and a bearing failure in the MD adherend, as shown in Fig. 15 (d).

The results of the experiments with the loading–unloading-reloading cycles are shown in Fig. 19. The delayed recovery deformation of the MD-ADP hybrid joint was slightly less than that of the corresponding ADP bonded joint since the deformation at unloading was less and recovery may have been restricted by bolt friction.

The effects of the displacement rate on the load–displacement responses of MD-ADP hybrid joints are shown in Fig. 20. Similarly to the ADP bonded joints (Fig. 11), the curves were shifted upwards at a higher rate, i.e. the yield and ultimate failure loads were increased

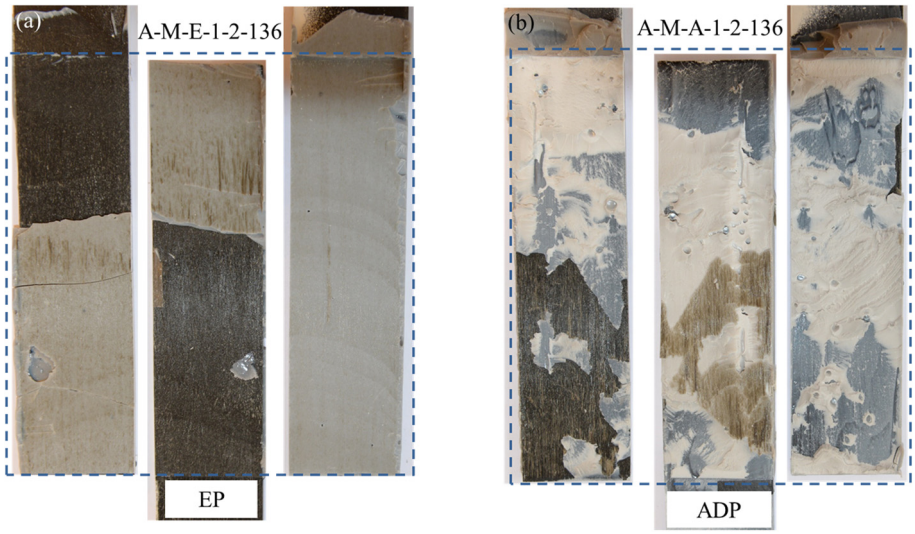


**Fig. 13.** Failure modes for 136-mm adhesive overlap length: (a) mixed adhesive/light-fiber-tear failure for EP joints; (b) mixed cohesive/light-fiber-tear failure for ADP joints.

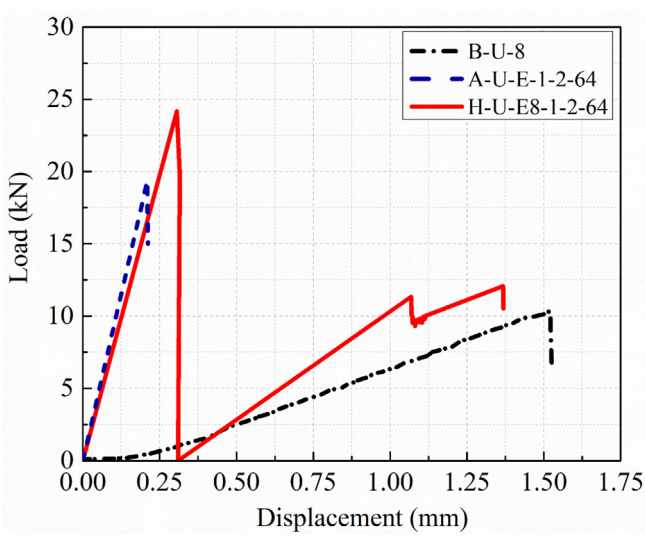


**Fig. 14.** Load-displacement responses of UD bolted, EP bonded and UD-EP hybrid joints.

due to the corresponding increases in the bonded connections. The yield and ultimate failure displacements were again not significantly affected by the displacement rate since they were dependent on the adhesive connection. After failure of the latter, the behavior of the remaining bolted connection was independent of the rate since the viscoelastic response of the much stiffer adherend matrix was much lower than that of the flexible adhesive.

## 4. Joint ductility and efficiency

Viscoelastic materials, such as the ADP adhesive and FRP adherends' epoxy matrix, have the ability to store and dissipate energy under load owing to their viscous properties, as shown in Fig. 21 [31]. The elastic energy, $W_e$, is released upon instantaneous unloading while inelastic energy can be dissipated by damage, $W_{d,dam}$, and internal friction (hysteretic energy), $W_{d,hyst}$. An energy-based ductility index was proposed in [31], as being the ratio of the inelastic energy $W_d$ to the total energy $W_t$ as follows:

$$\mu = \frac{W_d}{W_t} = \frac{W_{d,hys} + W_{d,dam}}{W_e + W_{d,hys} + W_{d,dam}} \tag{2}$$

The ductility index was calculated according to Eq. (2) based on the unloading curves shown in Fig. 19. Since the elastic energies were very small, the fact that unloading did not occur exactly at the peak load but slightly earlier did not significantly affect the index values. All the MD bolted joints and bonded and hybrid joints comprising the ADP adhesive exhibited very high ductility indices of >90%, while the UD bolted and epoxy adhesive joints showed purely brittle behavior, as shown in Fig. 22.

Also shown in Fig. 22 is the joint efficiency, which is defined as the ratio of joint ultimate failure load to the failure load of the adherend's full cross section, i.e. the member resistance between joints. Highest joint efficiencies of 30–46% were obtained for the ADP adhesive and hybrid joints of 64-mm overlap length, whereby the efficiency was increased by increasing the displacement rate. The efficiency could be significantly improved by increasing the overlap length and number of bolts. In the case of ADP adhesive joints, the dependency was linear and a highest value of 64% was obtained for the 136-mm overlap length. A 100% efficiency could thus be obtained for an approximately 210-mm overlap length in the case of an ADP adhesive joint or an ADP hybrid joint with two 8-mm bolts and a length of approximately 150 mm, assuming that all the resistances can be linearly summed (and a displacement rate of 1 mm/min). The joints with the highest ductility and efficiency were thus the hybrid joints composed of MD adherends and ADP adhesive.

## 5. Design of hybrid joints

The new CEN/TC250 Technical Specification for the design of fiber-polymer composite structures [28] provides guidelines for the design of bolted, bonded (adhesive) and hybrid joints. According to this document (Subclause 12.4), a composite structure comprising adhesive joints shall be designed as fail-safe, i.e. joint failure shall not result in failure of the whole structure or critical parts thereof, and failure of an adhesive joint shall be considered as an accidental design situation (according to EN 1990 [32]). Concerning hybrid joints (Subclause 12.5), the resistances of the adhesive bond and bolting should not be summed, unless flexible adhesives are used and it is confirmed by testing that the resistances of the adhesive bond and bolting

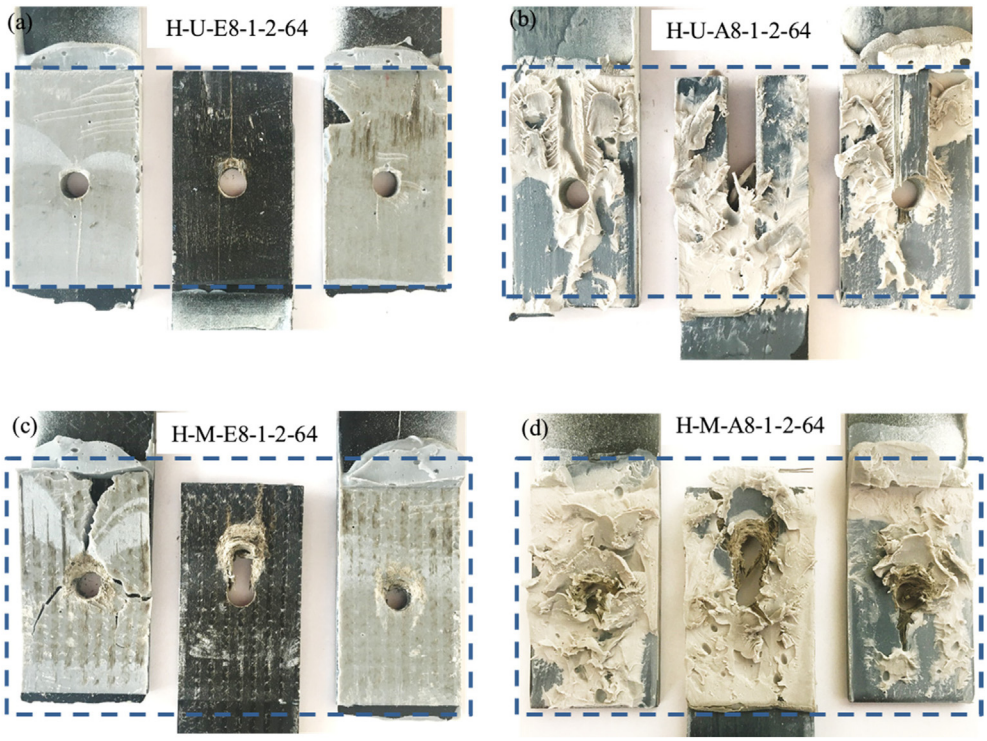


**Fig. 15.** Failure modes for hybrid joints: (a) UD-EP; (b) UD-ADP; (c) MD-EP; (d) MD-ADP.

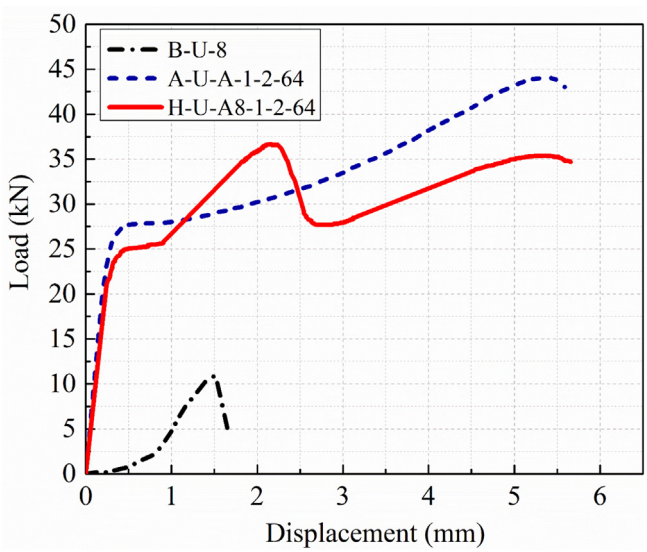


**Fig. 16.** Load-displacement responses of UD bolted, ADP bonded and UD-ADP hybrid joints.

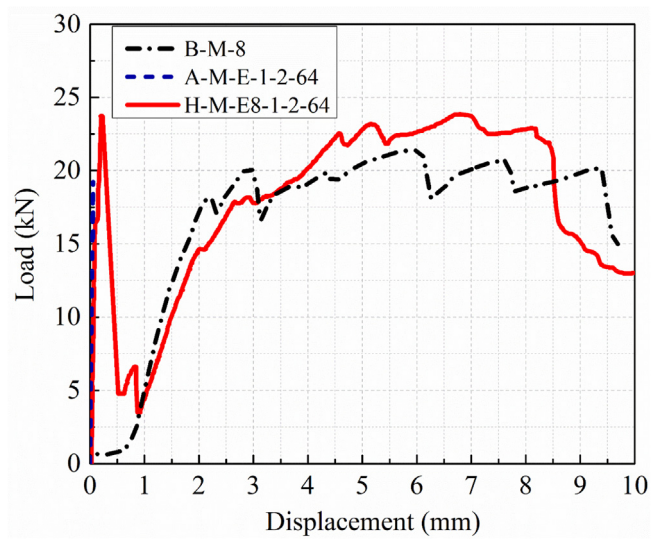


**Fig. 17.** Load-displacement responses of MD bolted, EP bonded and MD-EP hybrid joints.

can be summed. Furthermore, bolting may be used as a back-up system in adhesive joints to maintain the fail-safe condition.

MD-EP hybrid joints could thus fulfill those conditions. The individual resistances can however not be summed; the bolts can nevertheless be designed to act as back-up system to maintain the fail-safe condition. In the case of MD-ADP hybrid joints, as experimentally proved here, the resistances can be summed. The bolts can furthermore also be used as back-up system since, in an accidental design situation, they must bear only the dead load, which is normally small in lightweight composite structures. Furthermore, the bolts can also limit creep deformations in ADP adhesive layers to fulfill serviceability requirements. MD-ADP hybrid joints may also provide ductility and thus increase the overall safety of redundant engineering structures composed of brittle FRP members.

## 6. Conclusions

An experimental investigation of the load sharing of the bonded and bolted connection parts composing FRP hybrid joints was conducted. Amongst other things, the effects of fiber architecture, adhesive type, and displacement rate on the load-bearing behavior and ductility of bolted, bonded and hybrid joints were investigated. The conclusions of this work are summarized as follows:

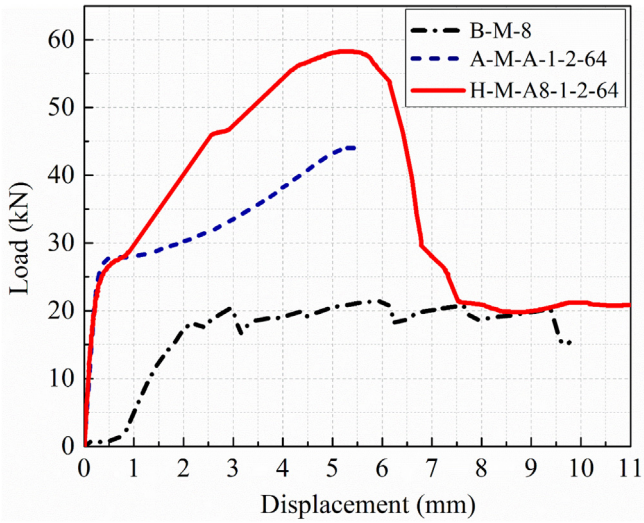


**Fig. 18.** Load-displacement responses of MD bolted, ADP bonded and MD-ADP hybrid joints.

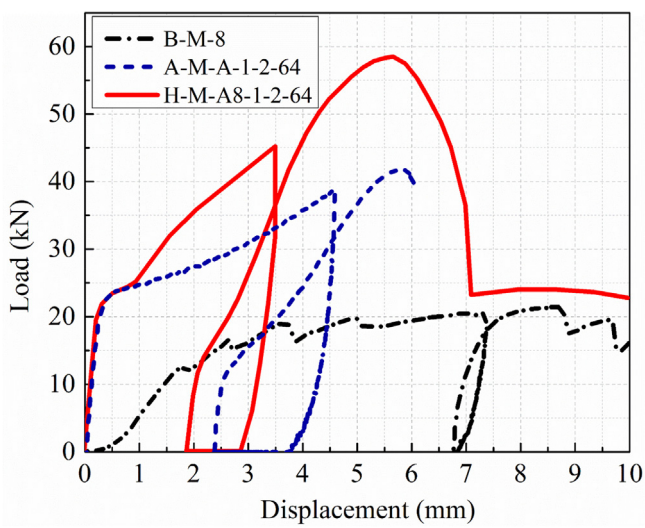


**Fig. 19.** Loading/unloading-displacement responses of MD bolted, ADP bonded and MD-ADP hybrid joints.

(1) Bolted joints with multidirectional (MD) fiber architecture significantly increased the joint resistance and deformation capacity compared to the unidirectional case due to a change of the failure mode from sudden splitting to progressive bearing failure.
(2) Bonded joints comprising flexible and ductile acrylic (ADP) adhesive exhibited a highly ductile response. Increasing the adhesive layer thickness of ADP joints resulted in almost proportionally increasing deformation. The resistance of ADP joints further increased almost linearly with the overlap length due to the uniform distribution of shear stresses along the adhesive layer.
(3) The resistance of hybrid joints comprising the ADP adhesive corresponded to the full summation of the resistances of the bonded and bolted connection parts due to almost equal and large deformation capacities.

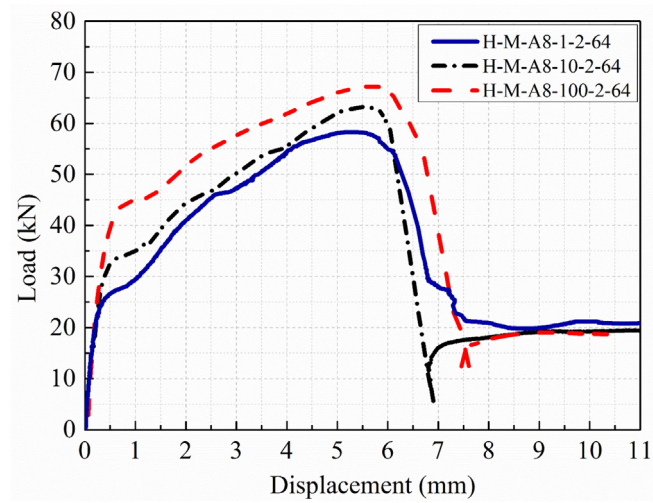


**Fig. 20.** Load-displacement responses of MD-ADP hybrid joints at different displacement rates.

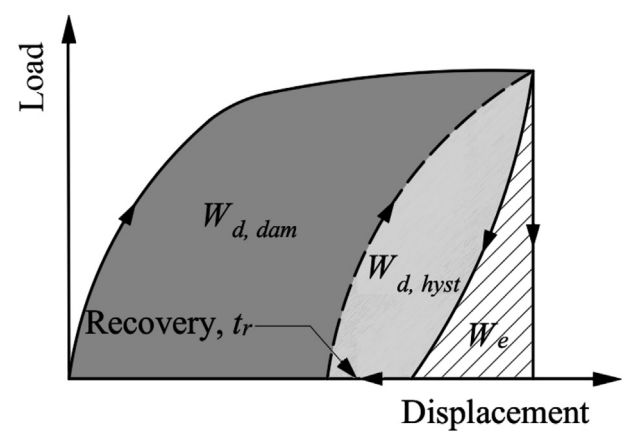


**Fig. 21.** Energy dissipation in viscoelastic materials [31].

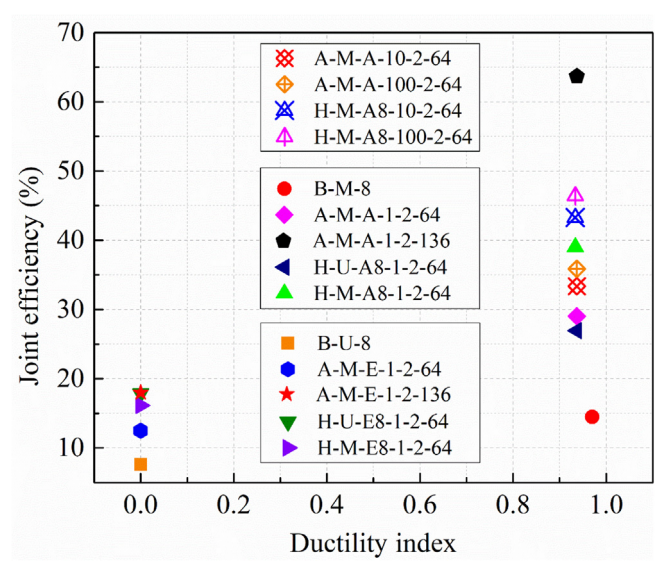


**Fig. 22.** Comparison of joint ductility and efficiency of bolted, bonded and hybrid joints.

(4) The yield and ultimate failure loads of ADP bonded joints and MD-ADP hybrid joints were significantly improved by increasing the displacement rate, while the deformation capacity was not decreased.
(5) All MD bolted joints and bonded and hybrid joints comprising the ADP adhesive exhibited high joint efficiencies and very high ductility indices of >90% and thus an excellent ability to dissipate inelastic energy.
(6) MD-EP and MD-ADP hybrid joints could fulfill fail-safe conditions as required in European standards. MD-ADP hybrid joints may further be implemented to provide ductility to engineering structures composed of brittle FRP members.

## 7. Data Availability Statement

The raw/processed data required to reproduce these findings cannot be shared at this time as the data also forms part of an ongoing study.

## CRediT authorship contribution statement

**Lulu Liu:** Investigation, Formal analysis, Writing - original draft. **Xin Wang:** Validation, Writing - review & editing, Funding acquisition. **Zhishen Wu:** Resources, Supervision. **Thomas Keller:** Conceptualization, Validation, Writing - review & editing.

## Declaration of Competing Interest

The authors declare that they have no known competing financial interests or personal relationships that could have appeared to influence the work reported in this paper.

## Acknowledgements

The authors gratefully acknowledge the financial support provided by the National Natural Science Foundation of China (No. 51878149), China; National Key Research and Development Program of China (No.2017YFC0703000), China; Postgraduate Research and Innovation Plan of Jiangsu Province (No.KYCX18_0110), Jiangsu Province, China and China Scholarship Council (No.201806090249), China. The authors also acknowledge Jiangsu GMV for providing BFRP pultrusions.

## References

[1] Wu Z, Wang X, Zhao X, Noori M. State-of-the-art review of FRP composites for major construction with high performance and longevity. Int J Sustain Mater Struct Syst 2014;1:201.
[2] Keller T. Recent all-composite and hybrid fibre-reinforced polymer bridges and buildings. Prog Struct Eng Mater 2001;3(2):132–40.
[3] Bakis CE, Bank LC, Brown VL, Cosenza E, Davalos JF, Lesko JJ, et al. Fiber-reinforced polymer composites for construction—State-of-the-art review. J Compos Constr 2002;6(2):73–87.
[4] Mosallam A. Design guide for FRP composite connections. Virginia: American Society of Civil Engineers; 2011.
[5] Keller T, Till V. Adhesively bonded lap joints from pultruded GFRP profiles. Part I: stress–strain analysis and failure modes. Compos Part B Eng 2005;36(4):331–40.
[6] Girão Coelho AM, Mottram JT. A review of the behaviour and analysis of bolted connections and joints in pultruded fibre reinforced polymers. Mater Des 2015;74:86–107.
[7] Bodjona K, Lessard L. Hybrid bonded-fastened joints and their application in composite structures: a general review. J Reinf Plast Compos 2016;35:764–81.
[8] Hart-Smith LJ. Bonded-bolted composite joints. J Aircr 1985;22:993–1000.
[9] Chan WS, Vedhagiri S. Analysis of composite bolted/bonded joints used in repairing. J Compos Mater 2001;35(12):1045–61.
[10] Kweon J-H, Jung J-W, Kim T-H, Choi J-H, Kim D-H. Failure of carbon compositeto-aluminum joints with combined mechanical fastening and adhesive bonding. Compos Struct 2006;75:192–8.
[11] Lopez-Cruz P, Laliberté J, Lessard L. Investigation of bolted/bonded composite joint behaviour using design of experiments. Compos Struct 2017;170:192–201.
[12] Fu MF, Mallick PK. Fatigue of hybrid (adhesive/bolted) joints in SRIM. Int J Adhes Adhes 2001;21:145–59.
[13] Clarke JL. Structural design of polymer composites: Eurocomp design code and background document. CRC Press; 2003.
[14] Keller T, Bai Y, Vallée T. Long-term performance of a glass fiber-reinforced polymer truss bridge. J Compos Constr 2007;11(1):99–108.
[15] Kelly G. Quasi-static strength and fatigue life of hybrid (bonded/bolted) composite single-lap joints. Compos Struct 2006;72:119–29.
[16] Hoang-Ngoc CT, Paroissien E. Simulation of single-lap bonded and hybrid (bolted/bonded) joints with flexible adhesive. Int J Adhes Adhes 2010;30:117–29.
[17] Bois C, Wargnier H, Wahl JC, Le Goff E. An analytical model for the strength prediction of hybrid (bolted/bonded) composite joints. Compos Struct 2013;97:252–60.
[18] Kelly G. Load transfer in hybrid (bonded/bolted) composite single-lap joints. Compos Struct 2005;69:35–43.
[19] Lim GH, Bodjona K, Raju KP, Fielding S, Romanov V, Lessard L. Evolution of mechanical properties of flexible epoxy adhesives under cyclic loading and its effects on composite hybrid bolted/bonded joint design. Compos Struct 2018;189:54–60.
[20] Raju KP, Bodjona K, Lim GH, Lessard L. Improving load sharing in hybrid bonded/bolted composite joints using an interference-fit bolt. Compos Struct 2016;149:329–38.
[21] Chen X, Zhang Y, Hui D, Chen M, Wu Z. Study of melting properties of basalt based on their mineral components. Compos Part B Eng 2017;116:53–60.
[22] Wu Z, Wang X, Wu G. Advancement of structural safety and sustainability with basalt fiber reinforced polymers. In: The sixth international conference on FRP composites in civil engineering (CICE, 2012.
[23] Liu L, Wang X, Wu Z, Keller T. Optimization of multi-directional fiber architecture for resistance and ductility of bolted FRP profile joints. Compos Struct 2020;248:112535.
[24] Anon. SikaFast 5221 NT fast curing 2-C structural adhesive. Technical data sheet Sika 2005.
[25] Anon. Sikadur-330, 2-component epoxy impregnation resin. Product data sheet. 2017.
[26] Angelidi M, Vassilopoulos AP, Keller T. Ductility, recovery and strain rate dependency of an acrylic structural adhesive. Constr Build Mater 2017;140:184–93.
[27] Keller T, Tirelli T. Fatigue behavior of adhesively connected pultruded GFRP profiles. Compos Struct 2004;65(1):55–64.
[28] CEN/TC 250. Design of fibre-polymer composite structures. Technical Specification, final draft, 30 October 2020.
[29] De Castro J, Keller T. Ductile double-lap joints from brittle GFRP laminates and ductile adhesives, Part I: experimental investigation. Compos Part B Eng 2008;39:271–81.
[30] Eslami G, Yanes-Armas S, Keller T. Energy dissipation in adhesive and bolted pultruded GFRP double-lap joints under cyclic loading. Compos Struct 2020;248:112496.
[31] Yanes-Armas S, de Castro J, Keller T. Energy dissipation and recovery in web-flange junctions of pultruded GFRP decks. Compos Struct 2016;148:168–80.
[32] EN 1990, Eurocode: Basis of structural design. European Committee for Standardization, Brussels; 2002.